product to the extent of ~60% as well as ~10% into recovered Leu-Tyr-NH_2 substrate.[29] Antonov has concluded that the fact ^{18}O is incorporated into the substrate "confirms the conclusion that pepsin catalysis follows the general-base mechanism".[28,29] There is however a mechanism, (Scheme III), which is a modification of that given by Hofmann, Dunn, and Fink,[4a] that would explain the above results and involves a transient anhydride intermediate that is rapidly cleaved by $H_2{}^{18}O$ specifically at the Leu C=O unit.[30] If the Leu CO_2H oxygens can tautomerically and positionally equilibrate, then such a process could account for the ^{18}O in the substrate and product and moreover does not place ^{18}O in the Asp-32 unit, since the same oxygen that attacks the Leu C=O is the one that departs. If we accept the Antonov results that indicate no ^{18}O is incorporated into the enzyme Asp units, then subsequent formation of an $Asp_{32}C(O)OC(O)Asp_{215}$ anhydride cannot occur since, in order for the enzyme to turn over, at least one $H_2{}^{18}O$ must be incorporated. If this is so, then the relevance of the subsequent formation of cyclic anhydrides from Ia to the enzymatic process is questionable. Nevertheless, the occurrence of the latter process in the hydrolysis of I does not invalidate a nucleophilic role for carboxylate in the enzyme.

Acknowledgment. We acknowledge the financial sources of the Natural Sciences and Engineering Research Council of Canada and the University of Alberta. J.K. thanks the NSERC for the award of a Summer Research Studentship.

Supplementary Material Available: Tables of second-order rate constants at various pH values for diacids II–VI with I, $T = 25$ °C, $\mu = 0.3$ (KCl) (4 pages). Ordering information is given on any current masthead page.

(20) The presence of succinic and glutaric anhydride was verified by comparison of the C=O stretching frequencies of authentic materials. In the case of the anhydride of *cis*-cyclopropane-1,2-dicarboxylic acid, FTIR analysis of authentic material confirms that the high-frequency band is a doublet at 1851 and 1868 cm^{-1}.

(21) As can be judged from Figure 4, acetate, malonate, and *trans*-cyclopropane-1,2-dicarboxylate are catalysts for the hydrolysis of I, but their mode of action is at present unknown.[6,10]

(22) (a) Kirby, A. J. *Adv. Phys. Org. Chem.* **1980**, *17*, 183–278. (b) Malonic anhydride has been synthesized by the ozonolysis of ketene dimer, but that is unstable above −30 °C: Perrin, C. L.; Arrhenius, T. *J. Am. Chem. Soc.* **1978**, *100*, 5249–5151.

(23) Kilpatrick, M., Jr. *J. Am. Chem. Soc.* **1928**, *50*, 2891.

(24) (a) Sachdev, G. P.; Fruton, J. S. *Proc. Natl. Acad. Sci. U.S.A.* **1975**, *72*, 3424–3427. (b) Medzihradszky, K.; Voynick, I. M.; Medzihradszky-Schweiger, M.; Fruton, J. S. *Biochemistry* **1970**, *9*, 1154–1162. (c) Pearl, L. in ref 1a, pp 189–195.

(25) For discussion of the pros and cons of enzyme binding inducing significant substrate strain or stress, see: (a) Fersht, A. R. *Enzyme Structure and Mechanism*, 2nd ed.; W. H. Freeman: San Francisco, 1985; pp 311–346. (b) Jencks, W. P. *Adv. Enzymol. Relat. Areas Mol. Biol.* **1975**, *43*, 219–410; **1980**, *51*, 75–106. (c) Palcic, M. M.; Klinman, J. P. *Biochemistry* **1983**, *22*, 5957–5966 and references therein.

(26) Accelerated hydrolysis of amides due to N-pyramidalization has been studied: Šlebocka-Tilk, H.; Brown, R. S. *J. Org. Chem.* **1987**, *52*, 805–808.

(27) (a) Takahashi, M.; Wang, T. T.; Hofmann, T. *Biochem. Biophys. Res. Commun.* **1974**, *57*, 39–46. (b) Wang, T. T.; Hofmann, T. *Biochem. J.* **1976**, *153*, 691–699.

(28) (a) Antonov, V. K.; Ginodman, L. M.; Rumsh, L. D.; Kapitannikov, Yu. V.; Barshevskaya, T. N.; Yavashev, L. P.; Gurova, A. G.; Volkova, L. I. *Bioorg. Khim.* **1980**, *6*, 436–446. (b) Antonov, V. K. in ref 1a, pp 202–220.

(29) Antonov, V. K.; Linsdman, L. M.; Rumsh, L. D.; Kapitannikov, Yu. V.; Barshevskaya, T. N.; Yavashev, A. G.; Gurova, A. G.; Volkova, L. I. *Eur. J. Biochem.* **1981**, *117*, 195–200.

(30) Extending this mechanism, it is now possible to explain why Antonov observed more than the expected 50% ^{18}O-incorporation in Leu-Leu.[29] If the initially cleaved anhydride (with one ^{18}O in Leu-COOH) re-forms the anhydride to a certain extent and is again cleaved by $H_2{}^{18}O$, then larger amounts than 50% are to be expected. Also, from this scheme it is possible to explain how the enzyme can act as an acyl-transfer or amino-transfer catalyst simply by postulating that either the initially produced acid or amine can leave the active site while its partner is retained.

Time-Resolved Proton–Phospholipid Interaction. Methodology and Kinetic Analysis

Esther Nachliel and Menachem Gutman*

Contribution from the Laser Laboratory for Fast Reactions in Biology, Department of Biochemistry, George S. Wise Faculty of Life Sciences, Tel-Aviv University, Tel-Aviv, Israel.
Received March 26, 1987

Abstract: The proton transfer between bulk and phospholipid surface was measured at real time by the laser induced proton pulse method. (Gutman, *Methods Biochem. Anal.* **1984**, *30*, 1–103). A pH indicator was adsorbed either on phospholipids–Brij-58 mixed micelles or on small unilamelar liposomes, and the protonation dynamics were recorded. The probe reactions are sensitive to the composition of the surface; its rate and extent of protonation vary with the surface density of the phospholipids and their pK. The observed transients were analyzed by numerical solution of coupled differential equations. The solution determines the rate constants of the phosphohead groups protonation and the rate they exchange protons with the probe. Through this analysis we can account for the capacity of the membrane to function as proton-collecting anthena; the protons first react with the acidic, ionized moieties on the surface and then, by rapid exchange, reach the strongest base on the surface. Both trapping capacity and rate of flux between surface groups are affected by the pK. Proton trapping is enhanced by less acidic lipids like phosphatidylserine (pK = 4.6). Proton mobility is enhanced by more acidic groups like phosphatidylcholine (pK = 2.2). This analysis predicts how combination of the two effects will determine apparent reactivity of a probe on phospholipid membrane.

The surface of the biomembranes is where most proton-transfer reactions take place. This region was in the center of interest for many years, but still we have very little information concerning the kinetic parameters associated with proton diffusion on the surface or between surface and bulk.

The understanding of the mechanism of proton transfer must stem from time resolved observations of proton diffusion between defined source and sink located in the precise position with respect to the membrane. The turnover of protogenic enzymes, like ATPase, is measured in milliseconds. Such enzymes are too slow

0002-7863/88/1510-2629$01.50/0

to be used for time resolved proton diffusion measurements.[1] Light triggers a proton release from photosynthetic systems, yet, the inherit complexity of the photosynthetic apparatus prohibits systematic study of proton-transfer reactions.[2] For example, a controlled variation of the phospholipids composition in a photosynthetic membrane cannot be achieved.

The laser induced proton pulse[3] is a combination of time resolved measuring techniques and analytical formalism which determines rate constants of diffusion-controlled proton-transfer reactions. The method was successfully used to investigate proton transfer in solutions or on interfaces, either in the absence or the presence of mobile buffer.[4-9]

Our previous studies were based on a simple, controlled model system. Neutral detergent micelles (Brij-58) were marked with two spectrally distinguishable indicators, and the effect of one on the protonation of the other was measured.[5] The analysis of the observation elucidated the role of immobile surface groups on the dynamic of protonation of other moities selected for observation.

In the present papers (see following paper in this issue, ref 7) we expand beyond the model studies, investigating proton transfer on liposomes and protein surface. The dynamics of protonation on such heterogeneous surfaces are determined by the reactivity of every surface group. The summation of all these interactions, through numerical solution of coupled nonlinear differential equations, reconstructs the observed phenomenon. The reaction of each surface group with H^+ is quantitated by rate constants specific for the interacting species. The determination of these rate constants and evaluation of their effects on the observed dynamics is the subject of the present paper. First we demonstrate how mixed micelles (Brij-58 plus phospholipids) can be used to determine the kinetic parameters of the phosphohead groups. Later we validate that the same rate constants are applicable for surfaces made of pure phospholipids. Finally we project from these measurements the general characteristics of proton transfer between bulk and phospholipid membranes.

Material and Methods

1. Instrumentation. Molectron UV 14 nitrogen laser was the source of a short excitation pulse (10 ns) delivering radiation at 337 nm at energy density of 0.5 M W/cm^2.

The excitation pulse was focused on the side of a four face quartz cuvette, and the irradiated sector was probed by a beam of the CW HeNe laser (632.8 nm). Energy transients of the monitoring light were amplified by a photomultiplier, digitized by a Biomation 8100 transient recorder, and accumulated by a Nicolet 1170 signal averagers. The content of the cuvette was constantly mixed by a small magnetic device, and its pH was monitored by a pH electrode.

2. Chemicals. Brij-58, phosphatidylcholine (egg yolk), phosphatidylserine, and phosphatidic acid were Sigma products. The proton emitters 2-naphthol and 2-naphthol-3,6-disulfonate were recrystallized before use.

No buffer was used throughout the experiment. The ionic strength was controlled by the addition of KCl.

3. Computations. The coupled nonlinear differential equations were solved numerically by the DVERK program of IMSL, by using a CDC 855 main frame computer. The differential equations are given in the appendix (for three variables) and in the appendix of ref 7 (for four variables). The latter equations were modified for phosphatidic acid computation by defining PAH^- = B, PA^{2-} = L, and LH = B.

4. An Analysis of the Results. The experimental system consisted of three reactants in aqueous solutions all in acid–base equilibrium: proton emitter (ROH), the pH indicator (HIn), and phospholipids (PL). The supporting micelles, made of Brij-58, are inert and do not participate in the acid–base reactions.

Scheme I

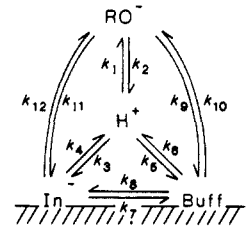

$$RO^- + H^+ \underset{2}{\overset{1}{\rightleftharpoons}} ROH \quad (1)$$

$$In^- + H^+ \underset{4}{\overset{3}{\rightleftharpoons}} HIn \quad (2)$$

$$PL^- + H^+ \underset{6}{\overset{5}{\rightleftharpoons}} PLH \quad (3)$$

$$In^- + HPL \underset{7}{\overset{8}{\rightleftharpoons}} HIn + PL^- \quad (4)$$

$$RO^- + HPL \underset{9}{\overset{10}{\rightleftharpoons}} ROH + PL^- \quad (5)$$

$$RO^- + HIn \underset{11}{\overset{12}{\rightleftharpoons}} ROH + In^- \quad (6)$$

The laser pulse excited the proton emitter to its first electronic singlet state, which due to its low pK (pK^* = 0.3),[3] discharges its proton. When the emitter relaxed to its ground state (less than 30 ns after the laser pulse), the ROH $\rightleftharpoons$ RO^- + H^+ system was poised in a state of disequilibrium.

Diffusion and collisional proton transfer propagates this perturbation to all other acid–base pairs. The experimental observation is the sum of all these reactions.

The purpose of our analysis is to extract from the observed transient the microscopic rate constants of each chemical reaction. These rate constants define the contribution of the corresponding reaction, at any given time, to the overall process.

The chemical reactions which we considered in our analysis include every possible reaction taking place between the ground-state reactants (see Scheme I).

At the time t = 0 reaction 1 is displaced from equilibrium by X_0, i.e., $[\overline{RO^-}]_0 = [\overline{RO^-}] + X_0$, $[\overline{H^+}]_0 = [\overline{H^+}] + X_0$, and $[\overline{ROH}]_0 = [\overline{ROH}] - X_0$. when $\bar{C}$ represents the equilibrium concentration. The transient X affects via reactions 2–6 all other acid–base equilibria.

The mathematical equivalent of the kinetics is the coupled nonlinear differential equations given in the Appendix. The first equation (dX/dt) includes the terms which control the relaxation of ROH to its prepulse concentration. The second equation (dY/dt) corresponds with the transient acidification of the indicator. The third one (dZ/dt) defines the transient acidification of the phospholipids.

The three equations are coupled, and the integral of (dY/dt) (the function Y versus time) corresponds with the dynamics of the probe. Upon insertion of the right parameters in the differential equations the function Y versus time will reproduce the experimental observations.

The solution of the Differential Equations. The differential equations given in the Appendix were integrated by the Dverk program. For integration we must determine the concentration of all reactants and the size of the initial perturbation (X_0) and replace the rate constants by their numerical values. The concentration of all reactants, dissociation constants, and pH are all known. The perturbation size (X_0) was determined for each set of the experiments.[3] Thus the unknown values are the rate constants. Some of these rate constants have been measured before by a simpler model systems.[9] These were taken in our calculations as constants. For superpositioning the Y versus time curve over the experimental results we had to vary only three or four rate constants.

Each of these rate constant was systematically varied within the range 10^7–10^{11} M^{-1} s^{-1}. The upper limit is for diffusion-controlled reaction of proton with small solutes. The lower one is for electrostatic-repulsed, steric-hindered diffusion-controlled reaction. Within this range we either varied systematically the rate constants or used the Minuit program with its "Simplex" algorithm to fit the Y versus time curve with the experimental dynamics (see Figures 6 and 3 of ref 7).

While this analysis is rather simple, it has the disadvantage of analyzing a single experiment. A more elegant procedure is to analyze simultaneously the results of many experiments. This type of analysis is based on measuring the dependance of the reactions macroscopic parameters on the initial conditions. The experimental curves are characterized by four macroscopic parameters: T_{max} and Y_{max} (the X and Y coordinates of the maximum) and two apparent rate constants γ_1 and γ_2.

(1) Schmidt, G.; Graber, P. *Biochim. Biophys. Acta* **1985**, *808*, 46–51.
(2) Polle, A.; Junge, W. *Biochim. Biophys. Acta* **1986**, *848*, 257–264.
(3) Gutman, M. *Methods Biochem. Anal.* **1984**, *30*, 1–103.
(4) Gutman, M.; Nachliel, E.; Gershon, E.; Giniger, R.; Pines, E. *J. Am. Chem. Soc.* **1983**, *105*, 2210–2216.
(5) Gutman, M.; Nachliel, E.; Giniger, R. *Eur. J. Biochem.* **1984**, *134*, 63–69.
(6) Nachiel, E.; Gutman, M. *Eur. J. Biochem.* **1984**, *143*, 83–88.
(7) Yam, R.; Nachliel, E.; Gutman, M. following paper in this issue.
(8) Gutman, M.; Nachliel, E.; Gershon, E. *Biochemistry* **1985**, *24*, 2937–2941.
(9) Gutman, M. *Methods Enzymol.* **1986**, *127*, 522–538.

Table I. The Rate Constants of Proton-Transfer Reactions on a Phospholipid Surface[a]

	reactive surface composition						
	1	2	3	4	5	6	7
	micell	mixed micell	mixed micell	liposome	liposome	mixed micell	liposome[c]
reaction	Brij	Brij + phosphatidyl-serine	Brij + phosphatidyl-choline	phosphatidyl-choline	phosphatidyl-choline + cholesterol	Brij + phosphatidyl acid	phosphatidyl-choline
$(RO^- + H^+)$ k_1	7×10^{10}	7×10^{10}	7×10^{10}	4.5×10^{10}	4.5×10^{10}	7×10^{10}	1×10^{10}
$(Ih^- + H^+)$ k_3	1×10^{10}	1×10^{10}	1×10^{10}	2.5×10^{10}	$2.7 \pm 0.2 \times 10^{10}$	1×10^{10}	$2.5 \pm 0.2 \times 10^{10}$
$PL + H^+$ k_5		$1.5 \pm 0.25 \times 10^{10}$	$0.75 \pm 0.25 \times 10^{10}$	$0.6 \pm 0.1 \times 10^{10}$	$0.6 \pm 0.1 \times 10^{10}$	$0.75 \pm 0.25 \times 10^{10}$	$0.6 \pm 0.1 \times 10^{10}$
$PLH + In^-$ k_5		1×10^{10}	1×10^{10}	1×10^{10}	1×10^{10}	1×10^{10}	1×10^{10}
$PLH + RO^-$ k_{10}		$5 \pm 0.4 \times 10^{8}$	$1 \pm 0.2 \times 10^{10}$	$1 \pm 0.3 \times 10^{10}$	$1 \pm 0.15 \times 10^{10}$	$2.5 \pm 1.1 \times 10^{8}$	1×10^{10}
$HIn + RO^-$ k_{12}	1×10^{7}	1×10^{7}	1×10^{7}	1×10^{7}	1×10^{7}	1×10^{7}	1×10^{10}
$PA^{2-} + H^+$ k'_5[b]						$3.5 \pm 0.25 \times 10^{9}$	
$PA^{2-} + HIn$ k'_8[b]						$1.5 \pm 0.25 \times 10^{6}$	
$PA^{2-} + ROH$ k'_{12}[b]						$6 \pm 0.5 \times 10^{8}$	
$PA^{2-} + PAk_2$ k_{18}[b]						1×10^{10}	
pK_1 (PL)		2.2 ± 0.1	2.2 ± 0.1	2.2 ± 0.1	2.2 ± 0.1	2.2 ± 0.1	2.2 ± 0.1
pK_2 (PL)		4.6 ± 0.5	—	—	—	8.0 ± 0.1	
$pK\ In^-$	5.4 ± 0.1	5.4 ± 0.1	5.4 ± 0.1	5.7 ± 0.1	5.2 ± 0.1	5.4 ± 0.1	5.7 ± 0.1
pK ROH	9.3	9.3	9.3	9.3	9.3	9.3	11.0

[a] The rate constants of collisional proton transfer are for the thermodynamic favored direction. The rates are expressed in $M^{-1}\ s^{-1}$ units. [b] See ref 11. [c] The proton emitter (β naphthol) is located on the liposomal surface.

(γ_1 is the first-order approximation for signal rise during the first 60% of amplitude; γ_2 is the first-order approximation for the first 60% of the decay.)

The measurements were carried out while modulating an external controllable variable (pH, reactant concentration, etc.). The dependence of the macroscopic parameters on this variable were drawn and compared with the dependence of the same parameter calculated for the computed Y versus time curves. We varied the unknown rate constants till the predicted dependence matched the experimental data (see Figures 2 and 4 of ref 5).

Acceptability of Solution. Three methods were used for determination of the rate constants. 1. A systematic search of the rate constants. 2. The Minuit program using "Simplex" algorithm for minimization of error. 3. Simultaneous fitting of the theoretical dependence of the macroscopic parameters on external variable (pH; $\bar{n}$) with the observed relationship.

The rate constants listed in Table I, were determined by either two or three methods, which converged into the same margin of uncertainty.

Results

Phospholipids–Detergents Mixed Micelles. Phospholipids have no physical property suitable for continuous monitoring of their state of protonation. Consequently their transient protonation must be deduced indirectly.

The system capable of providing this information is the rigorous numerical analysis of transient protonation of an indicator on a surface made of neutral detergent and phospholipids. Through the dynamics of the indicator we calculate the kinetic parameters of the phospholipid.

Typical transient protonation of such a system is demonstrated in Figure 1. The tracing represents the protonation of an indicator adsorbed on Brij-58 micelles (line A) and how phospholipids affect the dynamics (lines B–D). Phosphatidylcholine increases the protonation, while phosphatidylserine and phosphatidic acid decrease it.

The effect of each phospholipid will be presented below and analyzed.

Phosphatidylserine. Phosphatidylserine is a diprotoic acid, and both carboxyl and phosphomoiety can be protonated. Yet considering the fact that the phospho group is more acidic than the carboxyl and the probability of double protonation is nearly zero, we analyzed the results considering only the protonation of the carboxyl.

Figure 2 depicts the dependence of Y_{max} and γ_2 on the average content of phosphatidylserine in the micelle ($\bar{n}$).

The curves were obtained by assigning discreet values to each of the rate constants (k_5, k_8, and k_{10}) till the fit shown in the figure was obtained. These rate constants are listed in Table I column 2.

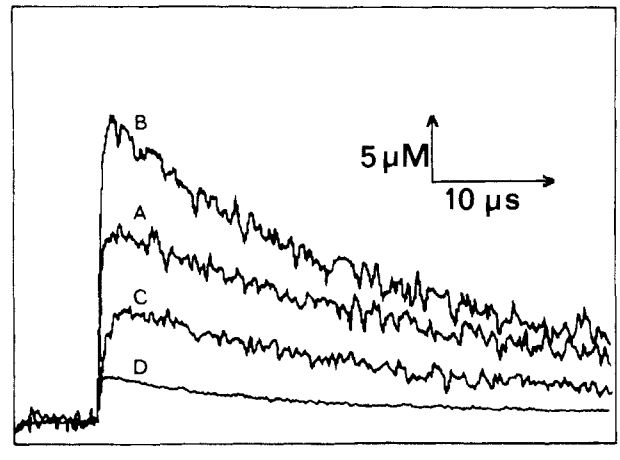

Figure 1. Transient protonation of bromocresol green adsorbed on mixed micelles. The reaction was carried out at pH = 7.3 ± 0.1 in a solution containing 500 μM bromocresol green, 1 mM of the proton emitter 2-naphthol-3,6-disulfonate, 500 μM micellar concentration of Brij-58 (40 mg/mL), and 3 mM of phospholipids. The transient protonation was measured at 633 nm through an optical path of 2.0 mm: (a) control, no phospholipid added (averaging of 256 events); (B) phosphatidylcholine (256 events); (C) phosphatidylserine (256 events); (D) phosphatidic acid (2098 events).

The shape of the lines as they are derived with other values of rate constants is shown in frames C and D.

The rate of phosphatidylserine protonation (k_5) (frames C and D, respectively) modulates both Y_{max} and γ_2 dependenc on $\bar{n}$. This rate is very crucial at low $\bar{n}$ values. It determines the augmenting effect of phosphatidylserine content on Y_{max}. Rates faster than 1.75×10^{10} increase the maximal protonation of the indicator detected at $\bar{n} \sim 1$ well above the experimental error. Slower rates of (1.25×10^{10}) flatten the curve below the experimental error. The dependence of γ_2 on $\bar{n}$ is steeper at low $\bar{n}$ values when k_5 is faster.

The rate of phosphatidylserine·H deprotonation by RO^- (k_{10}) causes the function γ_2 versus $\bar{n}$ to flare up. At low values of k_{10}, the curve reverses its direction (see frame E). The effect of k_{10} on Y_{max} versus $\bar{n}$ is hardly observed; the magnitude of Y_{max} is insensitive to k_{10} (not shown).

Apparently the rate of phosphatidylserine protonation modulates the probability that the proton will reach the indicator. On the other hand rapid deprotonation of phosphatidylserine·H accelerates the deprotonation of the indicator. This coupling between the indicator and lipid implies that they exchange protons between

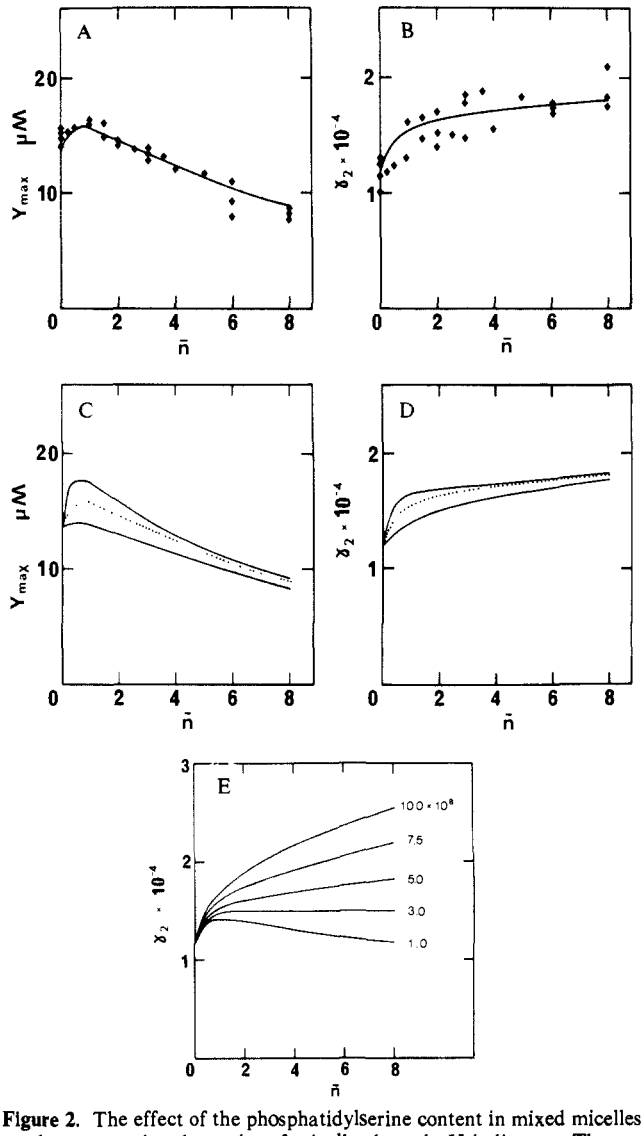

Figure 2. The effect of the phosphatidylserine content in mixed micelles on the protonation dynamics of micellar bound pH indicator. The experiments were carried out as in Figure 1, and the macroscopic parameters Y_{max} and γ_2 (see text for definition) were measured. (A) The dependence of Y_{max} on $\bar{n}$. The line drawn is the interrelation predicted by the rate constant listed in Table I column 2. (B) the dependence of γ_2 on $\bar{n}$. The line is the theoretical prediction. (C and D) The effect of k_5 on Y_{max} and γ_2, respectively. The functions were calculated for three values of k_5 5×10^{10} (top), 1.5×10^{10} (middle curve), and 5×10^9 (bottom). The middle dotted curves are identical with the lines drawn in frames A and B, respectively. (E) The effect of k_{10} on the dependence of γ_2 on $\bar{n}$. The values of k_{10} are marked in the figure. The middle line is identical with that drawn in frame B.

themselves (k_8) at a very fast rate. Indeed the shape of the initial protonation is very sensitive to k_8 (not shown).

Each of the rate constants modulates one or more macroscopic parameters of the observed transient. There is only one combination of rate constants which produces the fit shown in frames A and B.

Phosphatidylcholine. The protonation of phosphatidylcholine was measured by the same methods applied for phosphatidylserine. Figure 3 depicts the dependence of Y_{max} and γ_2 on $\bar{n}$. The lines shown are those predicted by the rate constants listed in Table I column 3.

These values were corroborated by a different experimental system, the analysis of protonation of an indicator adsorbed on phosphatidylcholine small unilamelar liposomes.

Unlike micellar systems, where the phospholipid surface density is a controllable variable, the phospholipid membrane is a homogeneous surface with constant head group density. By varying phospholipid concentration we do not affect the composition of

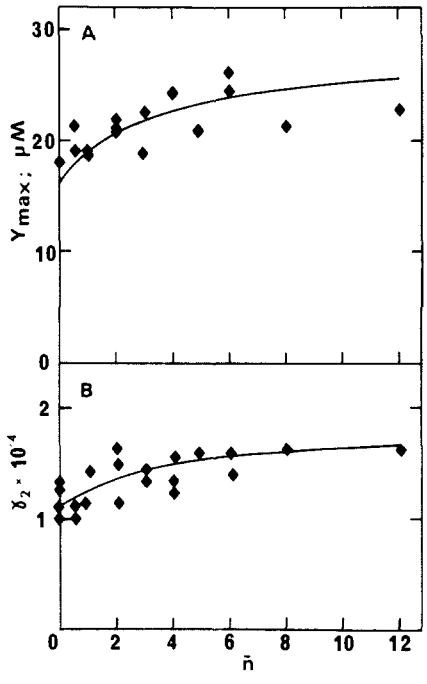

Figure 3. The effect of the phosphatidylcholine content in mixed micelles on the protonation dynamics of adsorbed pH indicator. The experiments were carried out and quantitated as described in Figure 2. The curves are the predicted dependence of Y_{max} (A) and γ_2 (B) on $\bar{n}$, as dictated by the rate constant listed in Table I column 3.

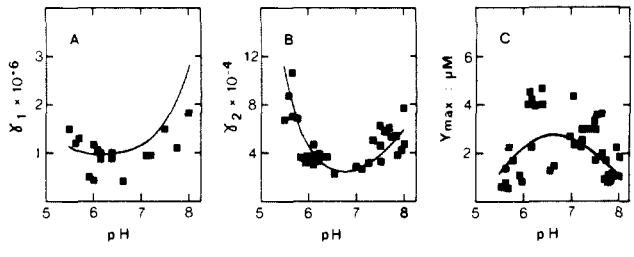

Figure 4. The effect of initial conditions (pH) on the protonation dynamic of bromocresol green adsorbed on phosphatidylcholine small unilamellar vesicles. The experiment was carried out with varying liposomal concentrations corresponding to 1–13 mg of phospholipids/mL, 1 mM 2-naphthol-3,6-disulfonate, and 50 μm bromocresol green. The parameters γ_1 (signal rise constant), γ_2 (signal decay), and Y_{max} were calculated from dynamic curves as in Figure 1. The continuous line is the curve predicted by the rate constants listed in Table I column 4.

the microenvironment near the indicator. This was experimentally observed. We could dilute the liposomal suspension between 13 mg of phosphatidylcholine to 1 mg/mL yet the macroscopic parameters of the indicator protonation γ_1, γ_2 and Y_{max} were invariable (the indicator concentration was constant). By varying the prepulse pH we obtained an independent variable affecting the macroscopic parameters (see Figure 4).

The lines drawn in the figure are an independent solution of the differential equations. The rate constants k_5, k_8, and k_{10} determined by these measurements are the same as obtained by the quantitative analysis of the experiments summarized in Figure 3 (see Table I columns 3 and 4). The difference between the two systems is expressed in the rate of the indicator protonation (k_3). On the liposomal surface the indicator is less screened by the polyoxyethylene chain of the detergent, and its rate of protonation increased by 2.5-folds. This accelerated protonation shifts the pK of the adsorbed indicator by 0.3 log units with respect to its value on Brij-58 micelles (5.7 versus 5.4, respectively).

Phosphatidylcholine and Cholesterol. Liposomes were made of phosphatidylcholine and cholesterol at a molar ratio of 4:1. Bromocresol green was adsorbed, and the vesicles were pulsed by protons discharged in the bulk. The numerical analysis (Figure 5) yielded the rate constants listed in Table I column 6. The rates

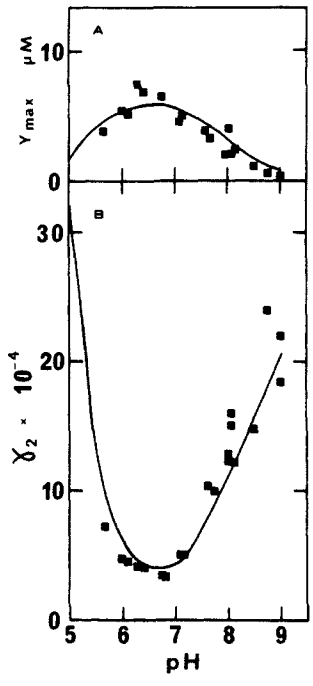

Figure 5. The effect of prepulse pH on the protonation dynamics of bromocresol green adsorbed in small unilamellar liposomes made of phosphatidylcholine and cholesterol at a molar ratio of 4:1: frame A, Y_{max} versus pH; frame B, γ_2 versus pH. The curves are the predicted functions with the rate constants listed in Table I column 5.

are not different from those measured in absence of cholesterol.

Phosphatidic Acid. Incorporation of phosphatidic acid into neutral micelles markedly decreases the amplitude of the measured protonation (Figure 6A) and accelerates the relaxation (Figure 6B).

The analysis of these experiments must consider the fact that phosphatidic acid has one acidic group with pK = 2.25 and another one more alkaline (pK = 8.0). As a result, at the experimental pH range, the most probable state of the phosphatidic acid will be PAH^-. This form can either accept a proton (like phosphatidylcholine) or donate a proton to RO^- generated by the pulse. The analysis of the experiments was carried out with four differential equations (see Appendix ref 7), calculating the integrals of ROH, HIn, PAH^-, and PAH_2.

The results of this treatment are represented by the lines drawn in Figure 6, and the rate constants are listed in Table I column 7.

The two protonation steps of phosphatidic acid differ not only by their pK values but also in their rate constants. All rates where PA^{2-} is protonated are significantly slower than the protonation of PAH^- (compare k_5 versus k'_5 and k_8 versus k'_8). The difference is definitely larger than the acceptable error. At present we have no explanation for this. It is very unlikely that the double-charged species is less exposed than PAH^-. Probably more intimate property of the immediate environment surrounding the phosphatidic acid head group must be invoked.

Proton Diffusion between Surface Sites. The experiments described above were initiated by protons homogeneously discharged in the bulk. In the experiment described below the protons were generated on the liposomal surface. The proton emitter β-naphthol was adsorbed on phosphatidylcholine liposomes, together with the indicator. We verified that under the experimental conditions given in the legend to Figure 7, the free reactants concentrations are less than 5% of the total. The average content, as calculated for the outer surface of the liposome, was 30–40 molecules of β-naphthol and six of the indicator. As the indicator cannot cross the membrane, protons discharged into the inner space of the liposomes are not detected. When adsorbed on a lipid interface only ~3% of the β-naphthol molecules are oriented in a position suitable for proton dissociation.[6] Thus, the pulse generated one to three protons on the outer surface of the liposome.

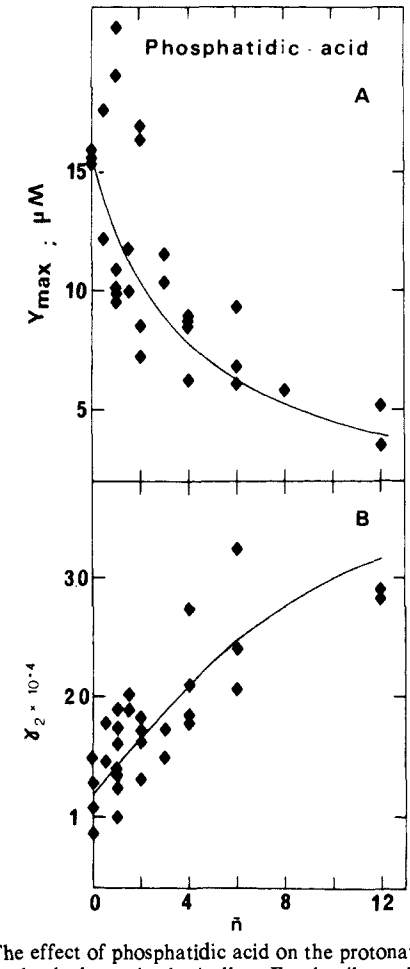

Figure 6. The effect of phosphatidic acid on the protonation dynamics of indicator adsorbed on mixed micelles. For details see Figure 2. The line was computed with the rate constants of Table I column 6.

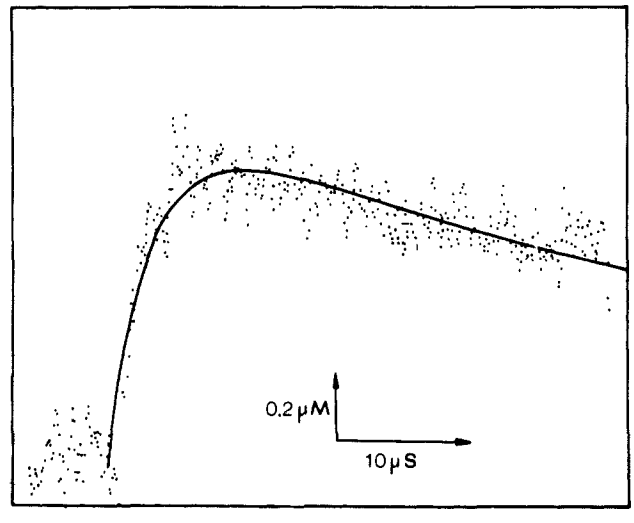

Figure 7. Dynamics of synchronized proton transfer from β-naphthol to bromocresol green both adsorbed into liposomal surface. The reaction was measured with phosphatidylcholine liposomes (13 mg/mL); 0.9 mM β-naphthol and 20 μM bromocresol green, pH 7.05. The signal was averaged for 256 pulses. The line was computed with the rate constants listed in Table I column 7.

The solution of such systems must use stochastic formalism,[6] but an approximative method can be used.[4] As discussed by Vass[10] an approximative nonstochastic solution will lead to an error of 15% (or less) in the rate constant. This approximation[4] substitutes

(10) Vass, S. *Chem. Phys. Lett.* **1980**, *70*, 135–137.

the proton-transfer reactions between surface groups by an equivalent second-order rate constant. This term (k_8) relates the nominal concentration of the surface groups with the velocity of the reaction. It has units of M^{-1} s^{-1} but does not represent a second-order reaction.

The continuous line going through the experimental points of Figure 7 is a numerical solution of the differential equations, with the rate constants appearing in Table I column 5. These values represent an independent solution of the equations, still they are identical (within uncertainity margin) with those determined by the systems corresponding with columns 3 and 4.

The rate of indicator protonation is similar to that measured with bulk proton donor and so is the rate of phosphatidylcholine protonation. The consistency of these values in the two systems clearly indicate that even if the proton is discharged on the surface its trajectory to other membranal components is passing through the water (in contrast to the conclusions drawn in ref 11).

The proton exchange between the surface groups k_8 (also k_{10} and k_{12} in presence of β-naphthol) all have the magnitude of 10^{10}. The meaning of this parameter will be discussed below.

Discussion

Critical Evaluation of the Rate Constants. The transient protonation which we investigated is a combination of many reactions proceeding simultaneously. Each reaction is characterized by its specific rate constants and is coupled, through common reactants, with other reactions. By the application of the numerical solution of the differential equation we could reconstruct each individual dynamics with a single set of rate constants.

There are two ambiguities which must be cleared: Does the rate constant constitute a single solution of the dynamics and what is the accuracy of these rate constants? The data presented can be reconstructed by only one set of rate constants, each defined by its inaccuracy limits. Considering the fact that the uncertainty range is rather narrow (in most cases less than factor of two), we regard the results as a single solution.

The integration procedure not only determines the unknown rate constants but also verifies those taken as known parameters. For example, without the correction of k_1 for the ionic strength effect (Table I column 4) whatever values we assigned to the unknown parameters (k_3, k_5, k_7, and k_{10}), the fit shown in Figure 4 could not be approached. Similarly, without considering reactions k'_5, k'_{10}, k'_{12}, and k_{18},[12] the reconstruction of the dynamics in the presence of phosphatidic acid was impossible.

The consistency of magnitude of the same rate constant, as measured for the different experimental systems (represented by the columns in Table I), corroborates the accuracy of the measurements and the analysis.

Bulk-Surface Proton Transfer. This subject is a key problem in modern bioenergetics and not free of some mystifying concepts. The experiments and analysis presented above provides a straightforward analysis of this phenomenon and is suitable for logical reconstruction of the reactions, all within the time frame of molecular events.

The charging of a surface with protons is a competition between two processes, recombination of protons with bulk anions versus their reactions with membrane bound groups. The outcome depends on the pK of the surface groups. A surface covered with low pK groups will retain proton for a very short period. The dwell time of proton on a phosphatidylcholine is $\tau_D(PC) = (k_5/K_{65})^{-1} \simeq 30$ ns. Within this time frame the compound will dissociate and the proton, diffusing to the bulk, will recombine with RO^-. The dwell time of proton on the carboxyl group of phosphatidylserine (pK_{65} = 4.6) is much longer, $\tau_D(PS) \simeq 4$ μs. The surface can be deprotonated not only by proton dissociation. A collisional proton transfer PLH + RO^- also takes place (k_{10}). The time constant for this reaction is $\tau_{Pt} = (k_{10}\cdot(RO^-))^{-1}$. In presence of 1 mM RO^-, the time constants for phosphatidylcholine and phosphatidylserine are 1 and 2, μs, respectively. It is quite obvious that deprotonation of phosphatidylcholine membrane will be mostly controlled by dissociation. The deprotonation of phosphatidylserine membrane will be dominated by collisional proton transfer.

These figures imply that the short-time state of protonation of membrane regions enriched by phosphatidylserine or phosphatidylcholine will respond differently to variation in buffer concentration or composition.

A proton attached to a surface can be transferred among the various groups. It is a sum of multiple dissociation–recombination steps. The high density of protonable groups on the surface ensures a high probability of multiple recombinations. The distance between the phospho moieties in phosphatidylcholine crystal is ~6 Å.[13] The distance between them on a bilayer surface is about the same.[13] Thus acidic groups on a phospholipid membrane are spaced at a distance comparable to the Coulomb cage radius (7 Å) of a monovalent ion.[14] A proton penetrating a Coulomb cage will be electrostatically attracted to the anion, at a force larger than the thermal energy. The recombination within the cage is extremely fast (~1 ns),[15,18] yet it may escape with a finite probability. A proton dissociating from one site will have a very high probability of stepping into the Coulomb cage of the nearby phosphate. Such repeated hopping between the cages will acquire the protons with high mobility, without impairing their fast equilibration with the bulk.

Proton translocation on the surface is affected by the pK of the surface groups. A short dwell time, as on phosphatidylcholine, encourages the proton to make, within a given time frame, many "hopping" steps. A less acidic surface like phosphatidylserine will delay the proton and suppress its mobility. These considerations furnish the microscopic mechanism for the effect of immobile buffers' pK on the apparent diffusion coefficient of protons, as formulated by McLaughlin and Junge.[19] A precise mathematical formulation of the proton diffusion on a surface, which accounts for the mechanism described above, will be unadvantageously complex. Instead we substituted it by apparent collisional proton transfer between the surface groups. For this reason the rate constants of these reactions do not have a physical meaning and cannot be compared with those reactions where one of the reactants is a free diffusing species.

The role of surface pK on proton binding capacity and agility are in accord with our experimental observation: the protonation dynamics of the same probe varies with the nature or composition of the phospholipid surface.

A condensed representation of this property is shown in the simulated dynamics given in Figure 8. We have plotted the projected time dependence of RO^- (A), HIn (B), and PSH (C) for protons interacting with an indicator on a membrane made of phosphatidylcholine and phosphatidylserine.

The continuous line represents a membrane of phosphatidylcholine marked with low concentration of bromocresol green. Such a membrane has a very low proton binding capacity, mostly that of the indicator. Because of that ~60% of the discharged protons will recombine, within 2 μs, with RO^- (line 1 in frame A). The rest will react with the indicator (frame B), except a minute fraction temporarily bound to PC (line 1 at bottom of frame A). Increasing the phosphatidylserine content of the membrane changes the scenario. The capacity of the membrane to compete for proton increases, and reprotonation of RO^- is delayed (lines 1–6 in frame A). At X_{ps} = 0.5 nearly 90% of the discharged

(11) Prats, M.; Tocanne, J. F.; Teissie, J. *Eur J. Biochem.* **1985**, *149*, 663–668.

(12) For definition of these rate constant see Scheme II in ref 7.

(13) Hauser, H.; Pascher, I.; Pearson, R. M.; Sundell, S. *Biochim. Biophys. Acta* **1981**, *650*, 21–51.

(14) Robinson, R. A.; Stokes, R. H. *Electrolyte Solutions*; Academic Press: New York, 1955.

(15) Pines, E.; Huppert, D. *J. Chem. Phys.* **1986**, *84*, 3576–3577.

(16) Agmon, N. *J. Chem. Phys.* **1985**, *82*, 2056–2066.

(17) Langhoff, C. A.; Moore, B.; DeMeuse, M. *J. Chem. Phys.* **1983**, *78*, 1191–1199.

(18) Mozumder, A. *J. Chem. Phys.* **1982**, *76*, 5107–5111.

(19) Junge, W.; McLaughlin, S. *Biochim. Biophys. Acta* **1987**, *890*, 1–5.

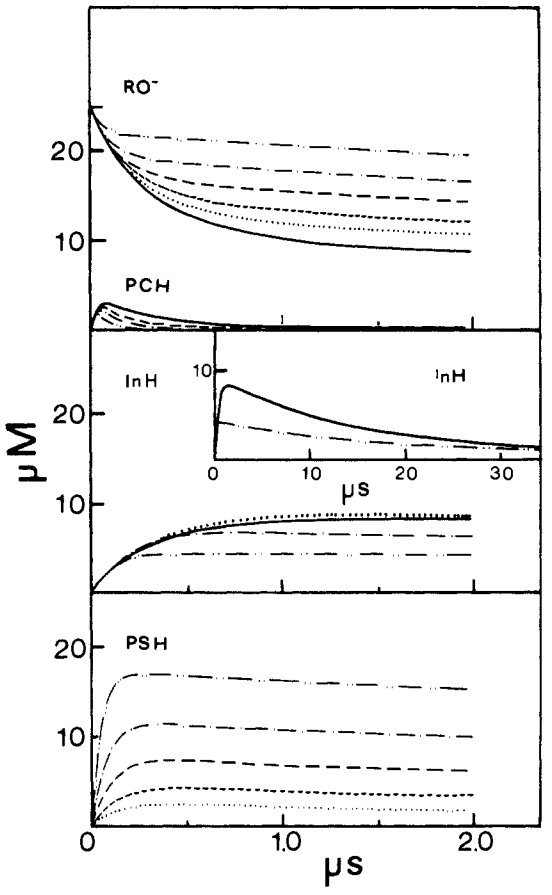

Figure 8. Simulated dynamics generated by a numerical solution of the differential equations describing bulk-surface proton transfer. The curves represent the state of protonation of each component in a system containing a pH indicator adsorbed on a phospholipid membrane made of phosphatidylcholine and phosphatidylserin at various proportions. Frame A depicts the relaxation of the proton emitter RO^- to its ROH state and the reversible protonation of the phosphatidylcholine. Frame B depicts the transient protonation of the adsorbed indicator, with insert showing the transient on longer time scale. Frame C depicts the transient protonation of phosphatidylserine. The mole fraction of phosphatidylserine is as follows: 1, $X_{ps} = 0$ (—); 2, $X_{ps} = 0.05$ (···); 3, $X_{ps} = 0.09$ (- - -); 4, $X_{ps} = 0.17$ (– –); 5, $X_{ps} = 0.28$ (–·–) and 6, $X_{ps} = 0.5$ (–···–). The computations were made for a system consisting of 1 mM phospholipids, 50 μM of adsorbed bromocresol green, 1 mM of 2-naphthol-3,6-disulfonate, 100 mM KCL with use of the differential equations given in the Appendix of ref 7.

protons are bound to the membrane.

Even low content of PS ($X_{ps} = 0.05$) already affects the protonation of the indicator (lines 1 and 2 frame B). The PS molecules increases the number of protons bound to the surface (line 2 in frame C), and the fast proton flux through the PC increases the protonation of the indicator. At high PS content ($X = 0.5$), nearly 66% of discharged protons react, within ~200 ns, with the PS. At such high content of phosphatidylserine the long dwell time of protons retards their mobility, and the protonation of the indicator decreases (lines 5 and 6 in frame B). A phosphatidylserine rich membrane has a large proton reservoir, and deprotonation of the indicator is compensated by protons from PSH. As a result the lifetime of HIn is prolonged from 16 μs in absence of PS to 22 μs (line 1 and 6 insert to Figure 8B).

Our experiments demonstrated that both time constants and protonation probability of a given group on a surface are grossly modulated by the nearby surface components. The mathematical analysis provided the physical rational for these observations. The application of this reasoning in the study of membrane bound proton driven enzymes will help to elucidate the intricate mechanism of their catalytic activity.

Acknowledgment. This research was supported by the American-Israeli Binational Science Foundation (84-100).

Appendix

The rate constants and reactants concentrations defined in Scheme I were combined in three coupled nonlinear differential equations.

The variables are X for incremental deprotonation of the proton emitter ($dX/dt = d[RO^-]/dt$), Y for incremental protonation of indicator ($dY/dt = d[HIn]/dt$), and Z the incremental protonation of the buffer (phospholipids in present case) (dZ/dt) = ($d[BH]/dt$).

$$\frac{dX}{dt} = a_{11}X + a_{12}Y + a_{13}Z + b_{11}X^2 + b_{12}XY + b_{13}XZ$$

$$\frac{dY}{dt} = a_{21}X + a_{22}Y + a_{23}Z + c_{22}Y^2 + c_{12}XY + c_{23}YZ$$

$$\frac{dZ}{dt} = a_{31}X + a_{32}Y + a_{33}Z + d_{33}Z^2 + d_{13}XZ + d_{23}YZ$$

where the terms a_{ij}, b_{ij}, c_{ij}, and d_{ij} are defined as follows

$$a_{11} = -k_1(\overline{H^+} + \overline{RO^-}) - k_2 - k_{10}\overline{BH} - k_9\overline{B^-} - k_{12}\overline{HIn} - k_{11}\overline{In^-}$$

$$a_{12} = (k_1 - k_{12})\cdot(\overline{RO^-}) - k_{11}(\overline{ROH})$$

$$a_{13} = (k_1 - k_{10})(\overline{RO^-}) - k_9(\overline{ROH})$$

$$b_{11} = -k_1;\ b_{12} = k_1 - k_{12} + k_{11};\ b_{13} = k_1 + k_9 - k_{10}$$

$$a_{21} = (k_3 - k_{11})\cdot(\overline{In^-}) - k_{12}\overline{HIn}$$

$$a_{22} = -k_3(\overline{In^-} + \overline{H^+}) - k_4 - k_8\overline{BH} - k_7\overline{B^-} - k_{11}(\overline{ROH}) - k_{12}(\overline{RO^-})$$

$$a_{23} = (k_8 - k_3)\cdot(\overline{In^-}) + k_7\overline{HIn}$$

$$c_{22} = k_3;\ c_{12} = k_{11} - k_3 - k_{12};\ c_{23} = k_7 - k_8 + k_3$$

$$a_{31} = (k_5 - k_9)(\overline{B^-}) - k_{10}(\overline{BH})$$

$$a_{32} = (k_7 - k_5)(\overline{B^-}) + k_8(\overline{BH})$$

$$a_{33} = -k_5(\overline{B^-} + \overline{H^+}) - k_6 - k_9(\overline{ROH}) - k_{10}(\overline{RO^-}) - k_7(\overline{HIn}) - k_8(\overline{In^-})$$

$$d_{13} = k_9 - k_5 - k_{10};\ d_{23} = k_8 - k_7 + k_5;\ d_{33} = k_5$$

Registry No. Brij-58, 9004-95-9; cholesterol, 57-88-5; bromocresol green, 76-60-8.